

## Theoretical models of double twinning in magnesium

Martina Ruffino <sup>\*</sup>*Department of Physics, King's College London, Strand, London WC2R 2LS, United Kingdom*Anthony T. Paxton *Department of Materials, Imperial College London, South Kensington Campus, London SW7 2AZ, United Kingdom  
and Department of Physics, King's College London, Strand, London WC2R 2LS, United Kingdom*

(Received 29 August 2023; accepted 19 October 2023; published 9 November 2023)

Satisfactory theoretical treatment of double twin growth has thus far not been achieved. Phenomenological theories of double twinning are based on the assumption that a double twin embryo grows on an invariant plane of the double twin transformation by means of a simple shear mechanism. We demonstrate the equivalence of A. G. Crocker's approach, which aims to identify the double twin invariant planes, and of later models of nonclassical twinning, which entail the use of correspondence matrices. These treatments, however, do not account for features of double twin growth observed in experiment, namely that this is a two-step process, where a primary twin forms fully before secondary twinning occurs internally. To resolve this conundrum, we introduce topological models of double twinning, which focus on the motion of twinning disconnections as the actors of twin growth. We first treat the case of secondary twinning disconnections interacting with a primary twin interface and calculate the magnitude of the resulting rotation of the habit plane; secondly, we model the interaction of secondary twinning disconnections with an array of primary twinning disconnections in the primary twin interface. We show that the latter model produces similar predictions for the double twin habit plane as those of the phenomenological theories, and we discuss validation of the topological models by experiment.

DOI: [10.1103/PhysRevMaterials.7.113603](https://doi.org/10.1103/PhysRevMaterials.7.113603)

### I. INTRODUCTION

Double twinning is defined as the internal, or secondary, twinning of a primary twin. In hcp metals, double twinning most often involves primary (compression) twinning on the  $\{10\bar{1}1\}$  or  $\{10\bar{1}\bar{3}\}$  planes and secondary (tension) twinning on the  $\{10\bar{1}2\}$  plane. This sequence, labeled compression-tension (C-T) double twinning, is the most commonly observed [1–3], but the opposite sequence, i.e., tension-compression (T-C) double twinning has also been reported [4,5]. The importance of double twinning as a deformation mode in magnesium is apparent, in particular with regards to its role in the formation of so-called “rare-earth texture” in magnesium alloys [6,7]; however, a comprehensive theoretical treatment of double twin growth and double twin interfaces has so far eluded the literature. Thus in this study we focus on theoretical models of double twinning in magnesium, with axial ratio  $\gamma = 1.624$ . Early so-called phenomenological theories of double twinning postulate that double twin transformations are described by equivalent simple shear modes, thus making double twinning a special case of nonclassical twinning. In contrast, topological models of double twinning focus on the interplay of

dislocations that accomplish the primary and secondary twin transformations, i.e., twinning disconnections. After introducing the classification of double twin variants in Sec. II, in Secs. III and IV we present the phenomenological and topological models of double twinning, respectively. We compare and contrast the two models in Sec. V A, and discuss experimental observations of double twins in Sec. V B.

### II. DOUBLE TWIN CLASSIFICATION

A given twinning mechanism is conventionally defined by specifying the twinning elements: these are  $K_1$  (the invariant plane),  $\eta_1$  (the shear direction),  $K_2$  (the second undistorted but rotated plane),  $\eta_2$  (the conjugate shear direction), and the plane of shear  $P$ . This characterization is, however, not unique, depending on the symmetry of the crystal: in the case of hcp crystals such as magnesium, each twin can be described equivalently by six sets of twinning elements. Thus, when two twinning mechanisms are combined in a double twin, 36 variants arise, conventionally named double twin types. For the double twinning sequences under consideration, only four variants are geometrically distinct, i.e., they produce reorientations of the basal pole by different angles. Formally, these are represented by the misorientation relations, that is by the operation required to bring the coordinate systems of the parent and double twin into coincidence,  $\mathbf{M}_{\text{tot}} = \mathbf{O}_f \mathbf{O}_i^{-1}$ , where  $\mathbf{O}_i$  and  $\mathbf{O}_f$  represent the initial and final orientations [2,3]. For a double twin, the initial orientation is taken to be the matrix and  $\mathbf{O}_i = \mathbf{I}$ , while the final orientation is given by applying the successive operations ascribed to each twinning

<sup>\*</sup>Corresponding author: [martina.ruffino@kcl.ac.uk](mailto:martina.ruffino@kcl.ac.uk)

Published by the American Physical Society under the terms of the [Creative Commons Attribution 4.0 International](https://creativecommons.org/licenses/by/4.0/) license. Further distribution of this work must maintain attribution to the author(s) and the published article's title, journal citation, and DOI.

event; these can be described as rotations of  $180^\circ$  about the  $\eta_1$  direction of each component twinning mode, expressed in their own coordinate systems, and are termed  $\mathbf{R}_A$  and  $\mathbf{R}_B$ . Hence, the total transformation, given in the coordinate system of the matrix, is

$$\mathbf{M}_{AB} = \mathbf{R}_A \mathbf{R}_B \mathbf{R}_A^{-1} \mathbf{R}_A = \mathbf{R}_A \mathbf{R}_B. \quad (1)$$

Thus the operation characterizing the double twin is obtained as a rotation matrix, from which the axis and angle of rotation can be extracted. Since the representation of such a rotation matrix is not unique due to symmetry, all equivalent descriptions of  $\mathbf{M}_{AB}$  are first obtained as the operations  $\mathbf{M}_{AB} \mathbf{D}_i$ , where  $\mathbf{D}_i$  is the set of proper symmetry operations of the crystal, and then the representation yielding the lowest rotation angle is chosen.

Out of the four geometrically distinct double twin variants available for each double twinning sequence examined here, we confine our discussion to those whose component twinning mechanisms present a common plane of shear, so-called types 1 and 2, in which case the misorientation relations can be represented as rotations about the normal to the plane of shear, i.e.,  $[1\bar{2}10]$ . Axis/angle pairs for the C-T double twins in magnesium (axial ratio  $\gamma = 1.624$ ) are the following:  $(10\bar{1}1) - (10\bar{1}2)$  type 1:  $-37.5^\circ[1\bar{2}10]$ ;  $(10\bar{1}1) - (\bar{1}012)$  type 2:  $-30.1^\circ[1\bar{2}10]$ ;  $(10\bar{1}3) - (\bar{1}012)$  type 1:  $-22.3^\circ[1\bar{2}10]$ ;  $(10\bar{1}3) - (10\bar{1}2)$  type 2:  $-29.7^\circ[1\bar{2}10]$ . It is easily shown that the misorientation relations for the opposite twinning sequences, i.e., T-C double twins, can be represented as rotations of the same magnitude as that of the corresponding C-T mechanism, but in the opposite direction.

### III. PHENOMENOLOGICAL THEORIES

Historically, classical deformation twins have been defined as those twins whose growth occurs via a simple shear mechanism on an invariant plane, producing a lattice whose orientation relative to the parent lattice is described by the classical orientation relations [8,9]. The notion of simple shear is retained in subsequent phenomenological theories of non-classical twinning, of which double twinning is described as a subclass, while discarding the requirement that only the classical orientation relations be obtained.

#### A. Crocker's theory of double twinning

The first theory of double twinning in a hcp metal was proposed by Crocker in 1962 [10], and its main postulate is that double twinning, as the combination of two simple shears, should also be represented by a simple shear. Then this treatment involves the identification of a plane left invariant by the two simple shears that characterize the primary and

secondary twinning modes, thus predicting the existence of a simple equivalent twinning mode describing the double twin transformation. In order to obtain a simple shear from the combination of two simple shears of the nondegenerate kind, where neither the  $K_1$  planes or the  $\eta_1$  directions of the two shears coincide, an additional rotation is to be allowed. In this way, any plane that has not been distorted by the action of the two simple shears may be rotated back to its original position, thus constituting an invariant plane. A further requirement that the shape change be homogeneous implies that the two component shears be coplanar, i.e., that the two twinning modes have the same plane of shear, and that both modes be compound. Hence our focus on type 1 and 2 double twin variants.

The matrix equation for a simple twinning shear  $\mathbf{S}$  of magnitude  $s$ , occurring on a plane with unit normal  $\mathbf{m}$  in the direction represented by the unit vector  $\boldsymbol{\ell}$  is given by

$$\mathbf{S} = \mathbf{I} + s\boldsymbol{\ell}\mathbf{m}^T. \quad (2)$$

We assign the subscripts  $A$  and  $B$  to the twinning elements of the primary and secondary twinning modes respectively. We choose the coordinate system where the  $z$  axis is the normal to the plane of shear, while the  $x$  and  $y$  axes are respectively the shear direction  $\eta_{1A}$  and the normal to the  $K_1$  plane of the primary twin. Since the plane of shear is common to the two twinning modes, we can omit the third index of each vector, and we write down the shears as two-dimensional matrices,

$$\mathbf{S}_A = \begin{pmatrix} 1 & s_A \\ 0 & 1 \end{pmatrix}, \quad (3)$$

$$\mathbf{S}_B = \begin{pmatrix} 1 - s_B \sin \alpha \cos \alpha & s_B \cos^2 \alpha \\ -s_B \sin^2 \alpha & 1 + s_B \sin \alpha \cos \alpha \end{pmatrix}. \quad (4)$$

Here,  $s_A$  and  $s_B$  are the twinning shears of the primary and secondary twin, respectively, and  $\alpha$  is the angle between the primary and secondary  $K_1$  planes. Finding the undistorted planes of the equivalent twinning mode amounts to finding vectors left undistorted by  $\mathbf{S}_B \mathbf{S}_A$ : such a vector, labeled  $\mathbf{r}$ , has its length unchanged by the transformation, such that the resulting vector  $\mathbf{q} = \mathbf{S}_B \mathbf{S}_A \mathbf{r}$  satisfies

$$\mathbf{q}^T \mathbf{q} = \mathbf{r}^T \mathbf{S}_A^T \mathbf{S}_B^T \mathbf{S}_B \mathbf{S}_A \mathbf{r} = \mathbf{r}^T \mathbf{r}. \quad (5)$$

Although the length of  $\mathbf{r}$  is unaltered by the shears, its direction will change; therefore, a rotation  $\mathbf{R}_C$  is added to the transformation in order to restore  $\mathbf{q}$  to the initial position, such that the total deformation is given by

$$\mathbf{S}_C = \mathbf{R}_C \mathbf{S}_B \mathbf{S}_A. \quad (6)$$

Taking  $\mathbf{r} = [\cos \phi, \sin \phi]$  to make an angle  $\phi$  with the  $x$  axis, i.e., with the primary  $K_1$  plane, Eq. (5) can be solved for  $\phi$ , such that two solutions are obtained,

$$\cot \phi = \frac{[s_B(\cos \alpha - s_A \sin \alpha) - D] \pm \sqrt{s_A s_B + s_A s_B D \sin \alpha + D^2}}{s_B \sin \alpha}, \quad D = \frac{s_A - s_B}{s_B \sin \alpha - 2 \cos \alpha}. \quad (7)$$

Since the planes defined by  $\phi$  and the normal to the plane of shear are left invariant by  $\mathbf{S}_C$ , which is itself a simple shear, they constitute the  $K_1$  and  $K_2$  planes of the equivalent simple twinning mode corresponding to double twinning. Therefore, the double twinning shear is given as a function of the angle  $\omega$  between  $K_1$  and  $K_2$  as

$$G = 2 \cot \omega = \sqrt{s_A s_B (s_A \sin \alpha - 2 \cos \alpha)(s_B \sin \alpha - 2 \cos \alpha) + (s_A - s_B)^2}. \quad (8)$$

Equations (7) and (8) can then be used to define a double twinning mode. Moreover, an expression for the rotation  $\mathbf{R}_C$  needed to make  $\mathbf{r}$  truly invariant can be found. This is a rotation about the normal to the common plane of shear, and its magnitude  $\psi$  given by the angle through which  $\mathbf{r}$  is rotated by  $\mathbf{S}_B\mathbf{S}_A$ , such that

$$\begin{aligned} \cos \psi &= \mathbf{r}^T \mathbf{q} = \mathbf{r}^T \mathbf{S}_B \mathbf{S}_A \mathbf{r} \\ &= 1 - s_A s_B \sin \phi \sin \alpha \cos(\phi - \alpha) \\ &\quad + \frac{1}{2} [s_A \sin 2\phi + s_B \sin 2(\phi - \alpha)]. \end{aligned} \quad (9)$$

The relationship between the parent and doubly twinned crystal is thus fully defined.

For the double twin mechanisms under consideration, Crocker identifies a number of degeneracies, summarized by his reciprocal theorem. This states that double twinning mechanisms whose primary twinning shears are either the same or reciprocal to one another, with the same applying to the secondary twinning shears, belong to the same equivalent simple twinning mode. The reciprocal of the  $(10\bar{1}1)$  twinning mode is  $(10\bar{1}\bar{3})$ , and that of the  $(10\bar{1}2)$  twinning mode is  $(\bar{1}012)$ . Thus C-T type 1 and 2 double twin variants belong to the same equivalent simple twinning mode; T-C  $(10\bar{1}2) - (10\bar{1}1)$  type 1 and  $(10\bar{1}2) - (10\bar{1}\bar{3})$  type 2 variants result in the same mode, as do  $(\bar{1}012) - (10\bar{1}1)$  type 2 and  $(\bar{1}012) - (10\bar{1}\bar{3})$  type 1 variants.

The implications of the reciprocal theorem may be illustrated by taking the C-T mechanisms as an example. According to the convention used by Crocker, a positive twinning shear moves the positive side of the  $K_1$  plane to the right; then a reflection of a shear in any plane changes its direction, and hence the sign of the shear. Thus for the  $(10\bar{1}1) - (10\bar{1}2)$  mechanism, with  $\gamma = 1.624$  and  $\Lambda = \gamma\sqrt{2/3}$ ,  $s_A = \frac{\sqrt{2}(2\Lambda^2-3)}{4\Lambda} = 0.138$ ,  $s_B = \frac{2-\Lambda^2}{\sqrt{2}\Lambda} = 0.129$  and  $\alpha = \tan^{-1} \frac{-3\Lambda}{\sqrt{2}(3+3\Lambda^2)}$ . Then, Eq. (7) yields two solutions,  $\phi_1 = -8.9^\circ$  and  $\phi_2 = 88.5^\circ$ , while from Eq. (8) we find that the double twinning shear is  $G = 0.258$ . If the secondary twinning plane is substituted with its reciprocal, i.e., if we consider  $(10\bar{1}1) - (\bar{1}012)$  type 2, then  $s_A = -\frac{\sqrt{2}(2\Lambda^2-3)}{4\Lambda}$ ,  $s_B = -\frac{2-\Lambda^2}{\sqrt{2}\Lambda}$  and  $\alpha = \tan^{-1} \frac{-3\Lambda}{\sqrt{2}(3+3\Lambda^2)} - \cot^{-1} \frac{s_B}{2}$  yield the same  $\phi_1$ ,  $\phi_2$  and  $G$ . Turning to  $(10\bar{1}\bar{3}) - (10\bar{1}2)$ , the parameters are  $s_A = -\frac{\sqrt{2}(2\Lambda^2-3)}{4\Lambda}$ ,  $s_B = \frac{2-\Lambda^2}{\sqrt{2}\Lambda}$  and  $\alpha = \tan^{-1} \frac{-3\Lambda}{\sqrt{2}(3+3\Lambda^2)} - \cot^{-1} \frac{s_A}{2}$ , producing  $\phi_3 = -5.5^\circ$ ,  $\phi_4 = 77.2^\circ$  and  $G = 0.258$ .  $\phi_3$  and  $\phi_4$  are now the angles between the invariant planes and  $(10\bar{1}\bar{3})$ , whereas  $\phi_1$  and  $\phi_2$  are measured relative to  $(10\bar{1}1)$ . Making allowance for this, it is seen that  $\phi_1$  and  $\phi_4$  define the same plane  $C_1$ , while  $\phi_2$  and  $\phi_3$  both define  $C_2$ . This corresponds to full verification of the reciprocal theorem. We thus assign the invariant plane defined by  $\phi_1$  to the  $(10\bar{1}1) - (10\bar{1}2)$  mechanism, and  $\phi_3$  to  $(10\bar{1}\bar{3}) - (10\bar{1}2)$ . The planes  $C_1$  and  $C_2$  can both be seen as  $K_1$  or  $K_2$  planes of the double twin transformation, such that the equivalent simple twinning mode is really two modes reciprocal to each other.

The features of the mode describing compression-tension double twinning are summarized in Table I. Here,

TABLE I. Features of the equivalent simple twinning mode describing double twinning in magnesium,  $\gamma = 1.624$ . The angles  $\phi$  and  $\psi$  are calculated using Eqs. (7) and (9), respectively, and they represent rotations about the normal to the  $(1\bar{2}10)$  plane of shear.

C-T DT	$(10\bar{1}1) - (10\bar{1}2)$ type 1	$(10\bar{1}1) - (\bar{1}012)$ type 2
$\phi$	$-8.9^\circ$	$-8.9^\circ$
Label	$C_1$	$C_1$
$K_1$	$(1.07, 0, -1.07, 0.70)$ $\approx (30\bar{3}2)$	$(1.07, 0, -1.07, 0.70)$ $\approx (30\bar{3}2)$
$\eta_1$	$[0.37, 0, -0.37, -1.14]$ $\approx [\bar{1}013]$	$[0.37, 0, -0.37, -1.14]$ $\approx [\bar{1}013]$
$\psi$	$0.4^\circ$	$-7.0^\circ$
Mis. relation	$-37.1^\circ[1\bar{2}10]$	$-37.1^\circ[1\bar{2}10]$
C-T DT	$(10\bar{1}\bar{3}) - (10\bar{1}2)$ type 2	$(10\bar{1}\bar{3}) - (\bar{1}012)$ type 1
$\phi$	$-5.5^\circ$	$-5.5^\circ$
Label	$C_2$	$C_2$
$K_1$	$(0.84, 0, -0.84, -3.17)$ $\approx (\bar{1}014)$	$(0.84, 0, -0.84, -3.17)$ $\approx (\bar{1}014)$
$\eta_1$	$[-1.69, 0, 1.69, -0.90]$ $\approx [202\bar{1}]$	$[-1.69, 0, 1.69, -0.90]$ $\approx [202\bar{1}]$
$\phi$	$7.3^\circ$	$-0.1^\circ$
Mis. relation	$-22.4^\circ[1\bar{2}10]$	$-22.4^\circ[1\bar{2}10]$
T-C DT	$(10\bar{1}2) - (10\bar{1}1)$ type 1	$(\bar{1}012) - (10\bar{1}1)$ type 2
$\phi$	$9.5^\circ$	$5.8^\circ$
Label	$C_3$	$C_4$
$K_1$	$(0.81, 0, -0.81, 2.28)$ $\approx (50\bar{5}14)$	$(1.10, 0, -1.10, -1.80)$ $\approx (30\bar{3}\bar{4})$
$\eta_1$	$[1.22, 0, -1.22, -0.86]$ $\approx [30\bar{3}\bar{2}]$	$[-0.96, 0, 0.96, -1.18]$ $\approx [50\bar{5}\bar{6}]$
$\psi$	$-0.4^\circ$	$-7.7^\circ$
Mis. relation	$37.1^\circ[1\bar{2}10]$	$22.4^\circ[1\bar{2}10]$
T-C DT	$(10\bar{1}2) - (10\bar{1}\bar{3})$ type 2	$(\bar{1}012) - (10\bar{1}\bar{3})$ type 1
$\phi$	$9.5^\circ$	$5.8^\circ$
Label	$C_3$	$C_4$
$K_1$	$(0.81, 0, -0.81, 2.28)$ $\approx (50\bar{5}14)$	$(1.10, 0, -1.10, -1.80)$ $\approx (30\bar{3}\bar{4})$
$\eta_1$	$[1.22, 0, -1.22, -0.86]$ $\approx [30\bar{3}\bar{2}]$	$[-0.96, 0, 0.96, -1.18]$ $\approx [50\bar{5}\bar{6}]$
$\psi$	$7.4^\circ$	$0.1^\circ$
Mis. relation	$37.1^\circ[1\bar{2}10]$	$22.4^\circ[1\bar{2}10]$

Miller-Bravais indices for the habit planes  $C_1$  and  $C_2$  are calculated, as well as the corresponding shear directions. For each choice of habit, the other C plane corresponds to the  $K_2$  plane of the transformation, with the corresponding shear direction becoming  $\eta_2$ .

In Table I, the angle  $\psi$  indicating the magnitude of the rotation that is imposed on the doubly twinned crystal to ensure that the habit planes are truly invariant is calculated for each twinning mechanism using Eq. (9). In the ‘‘Mis. relation’’ rows of the table, these angles are then added to those defining the misorientation relation between the basal plane of the parent crystal and that of the double twins, reported in Sec. II. It is noted that mechanisms with the same habit plane, i.e., those defined as types 1 and 2, present the same misorientation relations after the rotation  $\mathbf{R}_C$  is applied. Therefore, these mechanisms are indistinguishable from each other in Crocker’s theory, and only one type of double twin with rational plane of shear exists for each primary  $K_1$  plane chosen. In other words, both for the case of the type 1 and type 2 double twin, a small nucleus of the primary twin retwins internally, and although this happens on different planes, the double twin embryo then expands into the parent on the habit plane  $C_1$  or  $C_2$ ; in addition, a rotation, which may be accommodated either in the parent or in the double twin, or shared between the two crystals, causes the relative orientation of the matrix and the double twin to be the same for both types. While the misorientation relations for the type 1 mechanisms are effectively unchanged by the added rotation, the type 2 double twins are reoriented by a more sizable amount: this result implies that only the misorientations of the type 1 mechanisms should be observed experimentally in double twins of a noticeable size. Moreover, Table I shows that  $\psi$  is larger for the type 2 mechanisms by an order of magnitude with respect to the type 1 mechanisms; this would then suggest that type 2 double twinning mechanisms for this equivalent twinning mode are less likely to occur, as they require more accommodation.

The case of T-C double twins may similarly be studied. The plane  $C_3$  is found to be the invariant plane for the  $(10\bar{1}2) - (10\bar{1}1)$  type 1 and  $(10\bar{1}2) - (10\bar{1}\bar{3})$  type 2 mechanisms, while  $C_4$  is the invariant plane of  $(\bar{1}012) - (10\bar{1}1)$  type 2 and  $(\bar{1}012) - (10\bar{1}\bar{3})$  type 1 variants, with  $G = 0.258$  in both cases. Notably, the simple equivalent twinning mode for T-C double twinning is closely related to that of C-T double twinning: indeed,  $C_3$  may be obtained by referring  $C_1$  to the coordinate system of the  $(10\bar{1}1) - (10\bar{1}2)$  double twin. This is because  $C_1$  is not a mirror plane of the bicrystal formed by the matrix and double twin (as is the case for classical twinning), and thus can be referred to using two sets of indices depending on which basis is chosen. This is similarly the case for  $C_2$  and  $C_4$ . The angles  $\phi$ , as well as the indices of the invariant planes and the corresponding shear directions are also summarized in Table I, along with the angles  $\psi$  rotated by the additional rotation  $\mathbf{R}_C$  necessary to restore the invariant plane to its initial position and the corresponding modified misorientation relations between parent and doubly twinned crystals. It can be seen that these misorientation relations mirror the ones obtained for the C-T mechanisms, with one notable difference: the  $(\bar{1}012) - (10\bar{1}1)$  type 2 mechanism shares its habit plane and misorientation relation with  $(\bar{1}012) - (10\bar{1}\bar{3})$  type 1, as they have the same primary twin; on the other hand,  $(10\bar{1}1) - (\bar{1}012)$  type 2 has the same habit and misorientation as  $(10\bar{1}1) - (10\bar{1}2)$  type 1. It follows that  $(\bar{1}012) - (10\bar{1}1)$  type 2 and  $(10\bar{1}1) - (\bar{1}012)$  type 2 no longer have the same misorientation relation, and the same is true for

$(10\bar{1}2) - (10\bar{1}\bar{3})$  type 2 and  $(10\bar{1}\bar{3}) - (10\bar{1}2)$  type 2. This is a consequence of the reciprocal theorem, because the mechanisms that share a habit plane are the ones with the same primary twinning mode and secondary twinning modes reciprocal of each other. Nonetheless, it is confirmed that while T-C double twins present habit planes distinct from those of C-T double twins, their misorientation relations differ only in the direction of rotation. Therefore, Crocker’s theory of double twinning predicts that only two misorientation relations may be measured in double twins with a common, rational plane of shear:  $37.1^\circ$  and  $22.4^\circ \langle 1\bar{2}10 \rangle$ .

## B. Nonclassical twinning

Crocker’s theory of double twinning focused on identifying an invariant habit plane on which the double twinning shear would occur, so that a double twin nucleus would grow on this plane. Bevis and Crocker [11,12] generalized this concept to include all nonclassical twinning modes, i.e., modes characterized by a simple shear that restores the lattice in a different orientation, without requiring that one of the standard misorientation relations of classical twinning be produced. Rather than focusing on the invariant plane of the transformation, Bevis and Crocker instead show that it is possible to characterize a nonclassical twinning mode solely by knowing its correspondence matrix. We recast the derivation, given by the original authors in tensor notation, in matrix form. This is also done by Christian and Mahajan [13], but care should be taken with a few mistakes that have persisted in the latest edition of Christian’s book [14], and which are here rectified.

We start with a lattice defined by a direct basis  $\mathbf{a}_i$ ,  $i = 1, 2, 3$ ; then, the reciprocal basis  $\mathbf{a}_i^*$  is related to the direct basis by the metric  $G_{ij} = \mathbf{a}_i \cdot \mathbf{a}_j$ ,  $G_{ij}^{-1} = \mathbf{a}_i^* \cdot \mathbf{a}_j^*$ . A simple shear of magnitude  $s$  on the plane of unit normal  $\mathbf{m} = m_i^* \mathbf{a}_i^*$  in the direction of the unit vector  $\boldsymbol{\ell} = \ell_i \mathbf{a}_i$  is given by Eq. (2); repeated indices are summed over according to the Einstein summation convention. Then  $\mathbf{m}^T \mathbf{G}^{-1} \mathbf{m} = 1$  and  $\boldsymbol{\ell}^T \mathbf{G} \boldsymbol{\ell} = 1$ . By applying this shear to a lattice vector  $\mathbf{x}$ , we obtain the vector  $\mathbf{y}$ ,

$$\mathbf{y} = \mathbf{S}\mathbf{x}. \quad (10)$$

But according to the definition of simple shear,  $\mathbf{S}$  must restore the original lattice in a new orientation, such that

$$\mathbf{y} = \mathbf{L}\mathbf{z}, \quad (11)$$

where  $\mathbf{L}$  is a rotation and the lattice vector  $\mathbf{z}$  is related to the original lattice vector  $\mathbf{x}$  by

$$\mathbf{z} = \mathbf{C}\mathbf{x}. \quad (12)$$

The matrix  $\mathbf{C}$  is called the correspondence matrix, and it follows from Eqs. (10)–(12) that

$$\mathbf{S} = \mathbf{L}\mathbf{C}. \quad (13)$$

It can be shown that the matrix  $\mathbf{C}$  is unimodular, i.e., that  $|\mathbf{C}| = \pm 1$  [13,15]. Multiplying both sides of Eq. (13) from the left by  $\mathbf{S}^T \mathbf{G}$  and using the identity  $\mathbf{L}^T \mathbf{G} \mathbf{L} = \mathbf{G}$  [16], we find

$$\mathbf{S}^T \mathbf{G} \mathbf{S} = \mathbf{C}^T \mathbf{G} \mathbf{C}. \quad (14)$$

We now seek to restrict the shears  $\mathbf{S}$  to those that satisfy Eq. 14. Substituting (2) into (14), we find

$$s^2 \mathbf{m} \mathbf{m}^T + s(\mathbf{G} \boldsymbol{\ell} \mathbf{m}^T + \mathbf{m} \boldsymbol{\ell}^T \mathbf{G} + \mathbf{I}) + \mathbf{G} - \mathbf{C}^T \mathbf{G} \mathbf{C} = \mathbf{X} = 0, \quad (15)$$

where the matrix  $\mathbf{X}$  has been defined for later use. Multiplying by  $\mathbf{G}^{-1}$  from the right and taking the trace, and remembering that the trace of a matrix product is invariant under cyclic permutations, we find a condition for the magnitude of the shear  $s$ ,

$$s^2 = \text{Tr}(\mathbf{C}^T \mathbf{G} \mathbf{C} \mathbf{G}^{-1}) - 3. \quad (16)$$

Using Eq. (15), the normal to the  $K_1$  plane  $\mathbf{m}$  and the shear direction  $\boldsymbol{\ell}$  can also be specified. We form the expression

$$2m_\alpha^* m_\beta^* X_{\alpha\beta} - m_\beta^{*2} X_{\alpha\alpha} - m_\alpha^{*2} X_{\beta\beta}, \quad (17)$$

where the summation convention is suspended for Greek indices, and equate it to zero; upon defining  $\mathbf{Y} = \mathbf{G} - \mathbf{C}^T \mathbf{G} \mathbf{C}$ , we obtain three quadratic equations for the indices of  $\mathbf{m}$ ,

$$Y_{\alpha\alpha} m_\beta^{*2} - 2Y_{\alpha\beta} m_\alpha^* m_\beta^* + Y_{\beta\beta} m_\alpha^{*2} = 0. \quad (18)$$

Then Eq. (18) can be solved for the ratios  $m_\alpha^*/m_\beta^*$ . In general, two solutions will be found for the invariant plane: these represent the  $K_1$  and  $K_2$  planes of the transformation.

Once  $\mathbf{m}$  and  $s$  have been determined using Eqs. (18) and (16), the indices of  $\boldsymbol{\ell}$  may be found by solving  $X_{\alpha\alpha} = 0$ , which follows from  $\mathbf{X} = 0$ , Eq. (15). On the other hand, equations similar to (18) can be found for  $\boldsymbol{\ell}$ . We start by inverting Eq. (14),

$$\mathbf{S}^{-1} \mathbf{G}^{-1} \mathbf{S}^{-T} = \mathbf{C}^{-1} \mathbf{G}^{-1} \mathbf{C}^{-T}. \quad (19)$$

Using  $\mathbf{S}^{-1} = \mathbf{I} - s \boldsymbol{\ell} \mathbf{m}^T$ , we find

$$s^2 \boldsymbol{\ell} \boldsymbol{\ell}^T - s(\mathbf{G}^{-1} \mathbf{m} \boldsymbol{\ell}^T + \boldsymbol{\ell} \mathbf{m}^T \mathbf{G}^{-1}) + \mathbf{G}^{-1} - \mathbf{C}^{-1} \mathbf{G}^{-1} \mathbf{C}^{-T} = \mathbf{W} = 0, \quad (20)$$

where  $\mathbf{W}$  has been defined. Multiplying from the right by  $\mathbf{G}^{-1}$  and taking the trace, another expression is obtained for  $s^2$ ,

$$s^2 = \text{Tr}(\mathbf{C}^{-1} \mathbf{G}^{-1} \mathbf{C}^{-T} \mathbf{G}) - 3. \quad (21)$$

Comparing Eqs. (16) and (21), we find that the correspondence matrix has to obey the condition

$$\text{Tr}(\mathbf{C}^T \mathbf{G} \mathbf{C} \mathbf{G}^{-1}) = \text{Tr}(\mathbf{C}^{-1} \mathbf{G}^{-1} \mathbf{C}^{-T} \mathbf{G}). \quad (22)$$

This condition is reported incorrectly in Christian and Mahajan [13] and Christian's *Theory of transformations in metals and alloys*, third edition [14]: In both cases, the right-hand side of Eq. (22) reads  $\text{Tr}(\mathbf{C}^{-T} \mathbf{G}^{-1} \mathbf{C}^{-1} \mathbf{G})$ , which is incorrect as the trace of a matrix product is only invariant under cyclic permutations. By forming an expression for  $\mathbf{W}$  and  $\boldsymbol{\ell}$  similar to (17) and defining  $\mathbf{Z} = \mathbf{G}^{-1} - \mathbf{C}^{-1} \mathbf{G}^{-1} \mathbf{C}^{-T}$ , we find three simultaneous equations for the indices of  $\boldsymbol{\ell}$ ,

$$Z_{\alpha\alpha} \ell_\beta^2 - 2Z_{\alpha\beta} \ell_\alpha \ell_\beta + Z_{\beta\beta} \ell_\alpha^2 = 0, \quad (23)$$

similarly to Eq. (18). It should be noted that as a consequence of the above mentioned error appearing in Christian's book, the matrix  $\mathbf{Z}$  is also defined incorrectly in that instance.

It has thus been proven that knowledge of the correspondence matrix is sufficient to fully specify a twinning mode. Moreover, Bevis and Crocker show that the correspondence's

inverse, transpose, and transposed inverse, i.e.,  $\mathbf{C}^{-1}$ ,  $\mathbf{C}^T$ , and  $\mathbf{C}^{-T}$ , also represent independent twinning modes, although closely related to one another.

From the treatment above it is now evident that double twinning as envisaged by Crocker in the form of an equivalent simple twinning shear is a special case of nonclassical twinning; this connection was formally made by Acton *et al.* [17]. We may write the primary shear  $\mathbf{S}_A$  in Eq. (6) as  $\mathbf{S}_A = \mathbf{L}_A \mathbf{C}_A$ . On the other hand,  $\mathbf{S}_B$  is referred to the coordinate system of the parent crystal, rather than that of the primary twin where it actually occurs, such that its form is more complicated. Then, if we label the basis of the primary twin  $P$ , we see that  $\mathbf{S}_B$  and  ${}^P \mathbf{S}_B$ , i.e., the form it takes when referred to the basis  $B$ , are related by the similarity transformation  $\mathbf{S}_B = \mathbf{L}_A {}^P \mathbf{S}_B \mathbf{L}_A^{-1}$ , where  ${}^P \mathbf{S}_B = {}^P \mathbf{L}_B {}^P \mathbf{C}_B$ . Then, Eq. (6) becomes

$$\mathbf{S}_C = \mathbf{L}_C \mathbf{C}_C, \quad (24)$$

$$\mathbf{L}_C = \mathbf{R}_C \mathbf{L}_A \mathbf{L}_B, \quad (25)$$

$$\mathbf{C}_C = {}^P \mathbf{C}_B \mathbf{C}_A. \quad (26)$$

Equation (24) is now in the same form as (13), and thus  $\mathbf{C}_C$  characterizes the equivalent simple twinning shear arising from the combination of two twinning modes: All properties of the double twinning mode can then be derived using this correspondence matrix, which in turn is specified by the correspondence matrices of the component twinning modes. Additionally, the misorientation relations derived using this method will naturally include the additional rotation  $\mathbf{R}_C$  necessary to restore the habit plane to its initial position and thus make it truly invariant. This formulation also provides the explicit proof of Crocker's reciprocal theorem, as classical twinning shears reciprocal to one another have the same correspondence matrix; then the correspondence matrix that characterizes the double twinning shear is left unchanged if either of the component modes used is exchanged for its reciprocal.

By restricting the magnitude of the twinning shear, Bevis and Crocker derived all the unitary correspondence matrices that are able to describe a valid relationship between lattice vectors of the parent and twinned crystals. For each of these matrices, by changing the positions and signs of the rows and columns of the matrix further unimodular matrices may be obtained; in the case of cubic crystals studied by Bevis and Crocker these variants of the correspondence matrix all describe the same unit cell, as a consequence of symmetry. However, for hexagonal crystals such as magnesium, each correspondence matrix has 36 crystallographically distinct variants. Thus, any of these variants may in principle describe an independent twinning mode.

Applying the theory described above to hcp crystals, we first see that the metric for the three-dimensional hexagonal system is given by

$$\mathbf{G} = \begin{pmatrix} 1 & -\frac{1}{2} & 0 \\ -\frac{1}{2} & 1 & 0 \\ 0 & 0 & \gamma^2 \end{pmatrix} a^2, \quad (27)$$

where  $a$  is the lattice constant. The 36 variants of the correspondence matrices that are distinct for the hexagonal system are found for each matrix  $\mathbf{C}$  listed by Bevis and Crocker [11]

in their Table II, as well as for  $\mathbf{C}^{-1}$ ,  $\mathbf{C}^T$ , and  $\mathbf{C}^{-T}$ . The matrices thus obtained are substituted into Eq. (22) and matrices that do not satisfy this equation are discarded. Solutions for  $\mathbf{m}$  and  $\ell$  are then found using Eqs. (18) and (11) respectively; pairs of solutions that satisfy  $\mathbf{m}^T \ell = 0$  are retained. The corresponding  $K_2$  plane and  $\eta_2$  direction may be found for each  $K_1 - \eta_1$  pair. This is done by first obtaining the contravariant normal

$$\epsilon_{ijk} = \begin{cases} 0, & \text{if } i = j \text{ or } j = k \text{ or } i = k, \\ \sqrt{|G_{ij}|}, & \text{if } (ijk) \text{ is a cyclic permutation of } (123), \\ -\sqrt{|G_{ij}|}, & \text{if } (ijk) \text{ is an anticyclic permutation of } (123), \end{cases} \quad (29)$$

where  $|G_{ij}|$  is the determinant of  $\mathbf{G}$ ; the same is valid for  $\epsilon_{ijk}^*$ , provided that  $|G_{ij}|$  is substituted with  $|(G^{-1})_{ij}|$  [9]. The Miller indices of the plane of shear are then given by  $p_i^* = G_{ij} p_j$ . A rotation of the vector normal to  $K_1$ , referred to real space, by  $\pi/2 - \cot s/2$  about  $\mathbf{p}$  produces a vector  $\mathbf{g} = g_i \mathbf{a}_i$  parallel to the conjugate shear direction  $\eta_2$ . The normal  $\mathbf{w}$  to the conjugate twinning plane  $K_2$  is finally given by the cross product of  $\mathbf{p}$  and  $\mathbf{g}$ , both referred to the direct lattice; similarly to Eq. (28),

$$w_i^* = \epsilon_{ijk} g_j p_k. \quad (30)$$

The solutions obtained for  $w_i^*$  and  $g_i$  are substituted into Eqs. (18) and (11) respectively, to check that a reciprocal mode of shear on the  $K_2$  plane in the  $\eta_2$  direction exists with the same magnitude of shear  $s$ ; if this is not the case, the relative correspondence matrix  $\mathbf{C}$  is discarded as one not producing a conventional twinning mode, i.e., we require that the nonclassical twinning modes obey the theory of reciprocal twinning, which, albeit being proven only for classical

to the plane of shear  $p_i$  as the cross product of  $\mathbf{m}$  and  $\ell$ , both referred to the reciprocal lattice; in component form, this is written as

$$p_i = \epsilon_{ijk}^* l_j^* m_k^* = \epsilon_{ijk}^* l_r G_{rj} m_k^*, \quad (28)$$

where  $\epsilon_{ijk}^*$  is the Levi-Civita tensor referred to the reciprocal basis, and repeated indices are summed over. In a nonorthonormal 3D coordinate system, this is given by

twinning orientation relations, is generally assumed to hold for any twinning mode [18,19].

In this way, first of all we find the classical twinning modes, which for magnesium,  $\gamma = 1.624$ , are the component modes of double twinning, i.e.,  $\{10\bar{1}1\}$  and  $\{10\bar{1}2\}$  twinning. These modes are described respectively by variants of the matrices 4.20 and 2.19 in Table II of Bevis and Crocker, i.e.,

$$\mathbf{C}_{4.20} = \frac{1}{4} \begin{pmatrix} 2 & 6 & 3 \\ 2 & \bar{2} & 1 \\ 0 & 0 & \bar{4} \end{pmatrix}, \quad (31)$$

$$\mathbf{C}_{2.19} = \frac{1}{2} \begin{pmatrix} 0 & 1 & 0 \\ 4 & 0 & 0 \\ 2 & 1 & \bar{2} \end{pmatrix}. \quad (32)$$

These correspondences predict correctly all the twinning elements  $K_1 K_2 \eta_1 \eta_2; s$ ; these are obtained as planes and directions expressed in the three-dimensional hexagonal basis, and when converted to the four-dimensional Miller-Bravais system they are given by

$$\mathbf{C}_{4.20}^T : \{10\bar{1}1\} \{10\bar{1}\bar{3}\} \{10\bar{1}\bar{2}\} \{30\bar{3}2\}; \frac{\sqrt{2}(2\Lambda^2 - 3)}{4\Lambda}, \quad (33)$$

$$\mathbf{C}_{2.19} : \{10\bar{1}2\} \{10\bar{1}\bar{2}\} \{10\bar{1}\bar{1}\} \{10\bar{1}1\}; \frac{\Lambda^2 - 2}{\sqrt{2}\Lambda}. \quad (34)$$

Now, according to the method by Acton *et al.* [17] detailed above, the correspondence matrices describing double twinning may be found using Eq. (26), as the products of the correspondence matrices of the component twinning modes. Both compression-tension and tension-compression double twinning can be described in this way, and we obtain

$$(10\bar{1}1) - (10\bar{1}2) \text{ DT} : \mathbf{C}_{C-T} = \mathbf{C}_{2.19} \mathbf{C}_{4.20}^T, \quad (35)$$

$$(10\bar{1}2) - (10\bar{1}1) \text{ DT} : \mathbf{C}_{T-C} = \mathbf{C}_{4.20}^T \mathbf{C}_{2.19}. \quad (36)$$

The connection between  $\mathbf{C}_{C-T}$  and  $\mathbf{C}_{T-C}$  can be readily established by remembering that the correspondence matrices in the matrix product are involutory: hence, Eq. (36) can be written as

$$\begin{aligned} \mathbf{C}_{T-C} &= \mathbf{C}_{4.20}^T \mathbf{C}_{2.19} = \mathbf{C}_{4.20}^{-T} \mathbf{C}_{2.19}^{-1} \\ &= (\mathbf{C}_{2.19} \mathbf{C}_{4.20}^T)^{-1} = \mathbf{C}_{C-T}^{-1}. \end{aligned} \quad (37)$$

TABLE II. Angles rotated through by the primary twin interface due to the impingement of a secondary twinning disconnection, for C-T and T-C double twin mechanisms. The rotation axis is the normal to the plane of shear ( $1\bar{2}10$ ). The results are given for  $\gamma = 1.624$ .

C-T DT	$(10\bar{1}1) - (10\bar{1}2)$ type 1	$(10\bar{1}1) - (\bar{1}012)$ type 2
$\phi$	$-0.7^\circ$	$6.6^\circ$
$\alpha$	$-18.8^\circ$	$74.9^\circ$
C-T DT	$(10\bar{1}\bar{3}) - (10\bar{1}2)$ type 2	$(10\bar{1}\bar{3}) - (\bar{1}012)$ type 1
$\phi$	$-7.1^\circ$	$0.3^\circ$
$\alpha$	$75.2^\circ$	$-11.1^\circ$
T-C DT	$(10\bar{1}2) - (10\bar{1}1)$ type 1	$(\bar{1}012) - (10\bar{1}1)$ type 2
$\phi$	$0.8^\circ$	$7.6^\circ$
$\alpha$	$18.8^\circ$	$-74.9^\circ$
T-C DT	$(10\bar{1}2) - (10\bar{1}\bar{3})$ type 2	$(\bar{1}012) - (10\bar{1}\bar{3})$ type 1
$\phi$	$-7.1^\circ$	$-0.3^\circ$
$\alpha$	$-75.2^\circ$	$11.1^\circ$

The inverse  $\mathbf{C}^{-1}$  of a correspondence matrix  $\mathbf{C}$  is shown by Bevis and Crocker to define an inverse shear  $\mathbf{S}^{-1}$  expressed in the coordinate system of the sheared lattice; then we see that Eq. (37) implies that in the coordinate system of the lattice sheared by the compression-tension transformation, the correspondence matrix of tension-compression twinning defines the inverse shear that restore the lattice sites to their original positions. This is exactly as found by Crocker [10] in his treatment of double twinning, see Sec. III A.

As was found in Crocker's case, however,  $\mathbf{C}_{C-T}$  and  $\mathbf{C}_{C-T}^{-1}$  define independent twinning modes when referred to the parent lattice, producing twinning elements with different indices. Albeit products of involutory matrices, the correspondence matrices  $\mathbf{C}_{C-T}$  and  $\mathbf{C}_{T-C}$  are not equal to their inverses (which would also make them equal to each other) and thus describe nonclassical twinning modes. In the Miller-Bravais coordinate system, the twinning elements  $K_1 K_2 \eta_1 \eta_2; s$  of the two modes are given by

$$\mathbf{C}_{C-T} : ("30\bar{3}2") ("1014") ["1013"] ["202\bar{1}"]; 0.258, \quad (38)$$

$$\mathbf{C}_{T-C} : ("50\bar{5}14") ("30\bar{3}4") ["30\bar{3}2"] ["505\bar{6}"]; 0.258, \quad (39)$$

where the indices and the shear magnitude are given for  $\gamma = 1.624$ , and indices in inverted commas indicate irrational indices approximated to the nearest integer. The  $K_1$  and  $K_2$  planes given above are the same as the habit planes predicted by Crocker and given in Table I, and represent the habits of modes with primary twinning mechanisms reciprocal of each other, as per the statement of the reciprocal theorem.

Finally, the misorientation relations for the double twinning modes defined by these correspondence matrices may be obtained using Eq. (24) and solving for  $\mathbf{L}_C$ . The descriptions of  $\mathbf{L}_C$  equivalent by symmetry are obtained via the proper point symmetry operations of the hexagonal lattice, and the minimum axis/angle pair is chosen. We then recover the misorientation relations found by Crocker and given in Table I for C-T and T-C double twinning respectively.

Thus, it is verified that Acton *et al.*'s [17] treatment of double twinning, based on Bevis and Crocker's [11,12] treatment of nonclassical twinning, is entirely equivalent to Crocker's earlier theory, if more general. According to these theories, a newly formed primary twin nucleus quickly retwins internally, becoming a double twin embryo, which then grows on an invariant habit plane of the transformation via a simple shear mechanism. Other than on the basis of the magnitude of the equivalent simple twinning mode, the feasibility of the double twin transformation is evaluated based on the magnitude and complexity of the lattice shuffles associated with it. Indeed, in the simple equivalent twinning modes found above for C-T and T-C double twinning in magnesium only one-eighth of the lattice points are sheared directly into position, and the rest must shuffle to restore the original lattice in a new orientation; additional atomic shuffles are needed when the atomic basis is introduced. This renders the double twinning transformation as a simple twinning mechanism considerably less likely to occur than either tension or compression twinning, in which one-half and one-fourth of the lattice points are sheared to twin positions respectively. In the following section, we see

how this problem is eliminated by treating double twinning using the topological theory.

#### IV. TOPOLOGICAL MODELS

The phenomenological theories of classical and nonclassical twinning are based on the notion of a homogeneous simple shear on an invariant plane, as was explained in the previous section. The literature has shown conclusively that the twinning transformation is produced by the motion of twinning dislocations gliding on the  $K_1$  plane [13]; these have been renamed twinning disconnections as they have both dislocation and step character [20]. Crucially, this deformation mechanism is inhomogeneous, and Pond *et al.* [21] have shown for the case of  $(10\bar{1}2)$  twinning that while the dislocation character of the disconnection, represented by the Burgers vector, accomplishes the shear part of the twinning transformation, the step associated with the disconnection, represented by the step height, is responsible for the atomic shuffles.

The topological model of interfacial defects [22–24] may be used to obtain the twinning disconnection associated with a given twin mechanism. This model involves the study of the symmetry group of a bicrystal, that is a composite of two crystals, often called  $\mu$  and  $\lambda$ , related by a transformation  $\mathbf{P}$ . The operation characterizing a given defect in a bicrystal interface is found by combining symmetry operations of the symmetry groups of the  $\mu$  and  $\lambda$  crystals that do not survive the creation of the bicrystal. When translations of the  $\mu$  and  $\lambda$  crystal lattices are not coincident the defect that arises is a dislocation, whose Burgers vector is given by the difference in the translation vectors  $\mathbf{t}(\mu)$  and  $\mathbf{t}(\lambda)$  expressed in the same coordinate system,  $\mathbf{b} = \mathbf{t}(\lambda) - \mathbf{P}\mathbf{t}(\mu)$ . Twinning disconnections belong to this class of defect, and their Burgers vectors are parallel to the shear direction  $\eta_1$ . The height of the associated step may also be found for a given  $K_1$  plane normal  $\hat{\mathbf{n}}$ : the translations  $\mathbf{t}(\lambda)$  and  $\mathbf{t}(\mu)$  produce steps of height  $h_\lambda = \hat{\mathbf{n}} \cdot \mathbf{t}(\lambda)$  and  $h_\mu = \hat{\mathbf{n}} \cdot \mathbf{t}(\mu)$  respectively, and the step height of the disconnection is given by the overlap step, i.e., the smaller of the two steps [20]. However, for a twinning disconnection, the step heights associated with  $\mathbf{t}(\lambda)$  and  $\mathbf{t}(\mu)$  are equal, such that either can be used as the step height for the disconnection.

As mentioned in Sec. II, in the case of twinning the transformation relating the parent and the twin may be represented as a rotation of  $180^\circ$  about the  $\eta_1$  direction,  $\mathbf{P} = \mathbf{R}$ . One can then show that the twinning disconnection associated with  $(10\bar{1}2)$  twinning has Burgers vector  $\mathbf{b} = \frac{2-\Lambda^2}{2+\Lambda^2}[10\bar{1}\bar{1}]$ , where  $\Lambda = \gamma\sqrt{2/3}$ , and a step height of two  $(10\bar{1}2)$  lattice planes [25]; for  $(10\bar{1}1)$  twinning, the Burgers vector of the disconnection is  $\mathbf{b} = \frac{2\Lambda^2-3}{2\Lambda^2+1}[10\bar{1}\bar{2}]$ , with a step height of four  $(10\bar{1}1)$  planes [26,27], while for the reciprocal  $(10\bar{1}\bar{3})$  mode the twinning disconnection burgers vector is  $\mathbf{b} = \frac{2\Lambda^2-3}{2\Lambda^2+9}[30\bar{3}2]$  and the step height is four  $(10\bar{1}\bar{3})$  planes. These are the twinning disconnections of the twinning mechanisms that make up the double twinning sequences of interest here, and they are thus used as the building blocks of the topological models presented in the following sections.

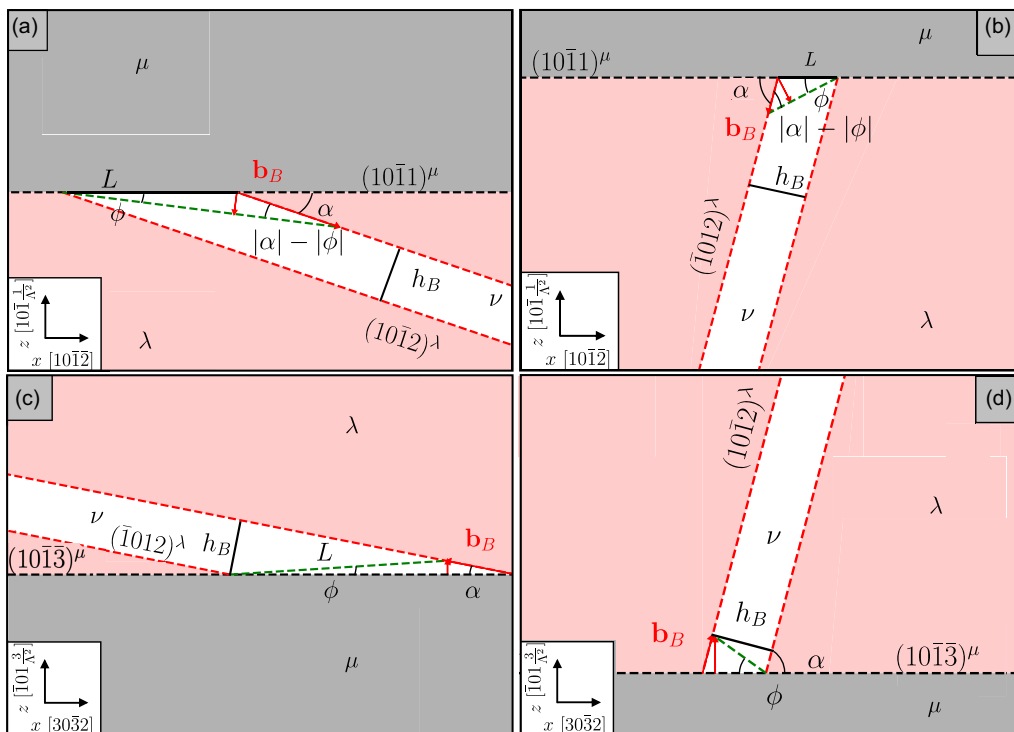


FIG. 1. Schematic of a secondary twinning disconnection with Burgers vector  $\mathbf{b}_B$  and step height  $h_B$  impinging on a flat primary twin interface. The parent, primary, and secondary twin are denoted respectively by  $\mu$ ,  $\lambda$ , and  $\nu$ . (a)  $(10\bar{1}1)^\mu - (10\bar{1}2)^\lambda$  type 1 double twin;  $L$  is the distance between the origin and the point where the top of the step meets the primary twin interface. (b)  $(10\bar{1}1)^\mu - (\bar{1}012)^\lambda$  type 2 double twin;  $L$  is as in (a). (c)  $(10\bar{1}3)^\mu - (\bar{1}012)^\lambda$  type 1 double twin;  $L$  (in green) is the distance between the origin and the tip of the Burgers vector. (d)  $(10\bar{1}3)^\mu - (\bar{1}012)^\lambda$  type 2 double twin;  $L$  (not labeled) is as in (c), in green.

### A. Disconnections impinging on a flat interface

In the first topological model of double twinning, we consider a fully formed primary twin with a flat commensurate interface along the  $K_1$  plane; we then take a secondary twinning disconnection to impinge on the primary twin interface. Assuming that the movement of atoms in the interface is not constrained by the material surrounding the twin, all the atoms encompassed by the length of the step are sheared by an amount corresponding to the Burgers vector of the secondary twinning disconnection; the next secondary twinning disconnection would then shear atoms by twice the Burgers vector, and so on. Thus the result is that the primary twin interface is overall rotated about the normal to the plane of shear common to the two twinning modes.

In order to illustrate this, we examine the case of C-T type 1 double twinning, with twinning sequence  $(10\bar{1}1)^\mu - (10\bar{1}2)^\lambda$ , where we have denoted the parent crystal by  $\mu$  and the primary twin by  $\lambda$ . Then the primary twin interface is the  $(10\bar{1}1)$  plane of the matrix, and the secondary twinning disconnections with Burgers vector  $\mathbf{b}_B$  and step height  $h_B$  glide on the  $(10\bar{1}2)$  plane of the primary twin. This situation is illustrated in Fig. 1(a), where the length of the Burgers vector relative to the step height has been exaggerated for clarity.

Seeking to calculate the angle  $\phi$  rotated through by the primary twinning plane as a result of the action of the secondary twinning disconnections, we label the angle between  $(10\bar{1}1)^\mu$  and  $(10\bar{1}2)^\lambda$   $\alpha$ , and  $L$  is the distance between the origin and

the top of the step. We then see that the component of  $\mathbf{b}_B$  (in red in the figure) perpendicular to the new habit plane, whose trace is given in green in the figure, makes up the short side of two triangles, one with hypotenuse  $L$  and the other with hypotenuse  $h_B$ . We can then write the equality

$$L \sin \phi = b_B \sin(|\alpha| - |\phi|), \quad (40)$$

where we have used the absolute values of the angles  $\alpha$  and  $\phi$  to make sure that the internal angles of all the triangles we use for trigonometric computation sum up to  $\pi$ . Using  $L = |h_B| / \sin |\alpha|$ ,  $|s_B| = b_B / |h_B|$  and solving for  $|\phi|$ , we find

$$|\phi| = \cot^{-1} \left( \frac{|s_B| \sin |\alpha| \cos |\alpha| - 1}{|s_B| \sin^2 |\alpha|} \right). \quad (41)$$

As we have obtained the absolute value of  $\phi$ , to ascertain its sign it is necessary to consider the sign of  $\alpha$  and the direction of the Burgers vector  $\mathbf{b}_B$ ; this can be done by observing Fig. 1(a): in this case, following the impingement of a secondary twinning disconnection the primary twinning plane undergoes a clockwise rotation, such that  $\phi$  is to be negative. Using Eq. (41) we obtain  $|\phi| = 0.7^\circ$ , and following the examination of the figure we find that the habit plane of the primary twin undergoes a rotation of magnitude  $\phi = -0.7^\circ$  as the double twin is formed.

The scenario examined above may also be considered in Crocker's simple shear framework. The angle  $\phi$  is then that by which the primary  $K_1$  plane is rotated by the secondary twinning shear  $S_B$ , which was defined by Eq. (4). The unit

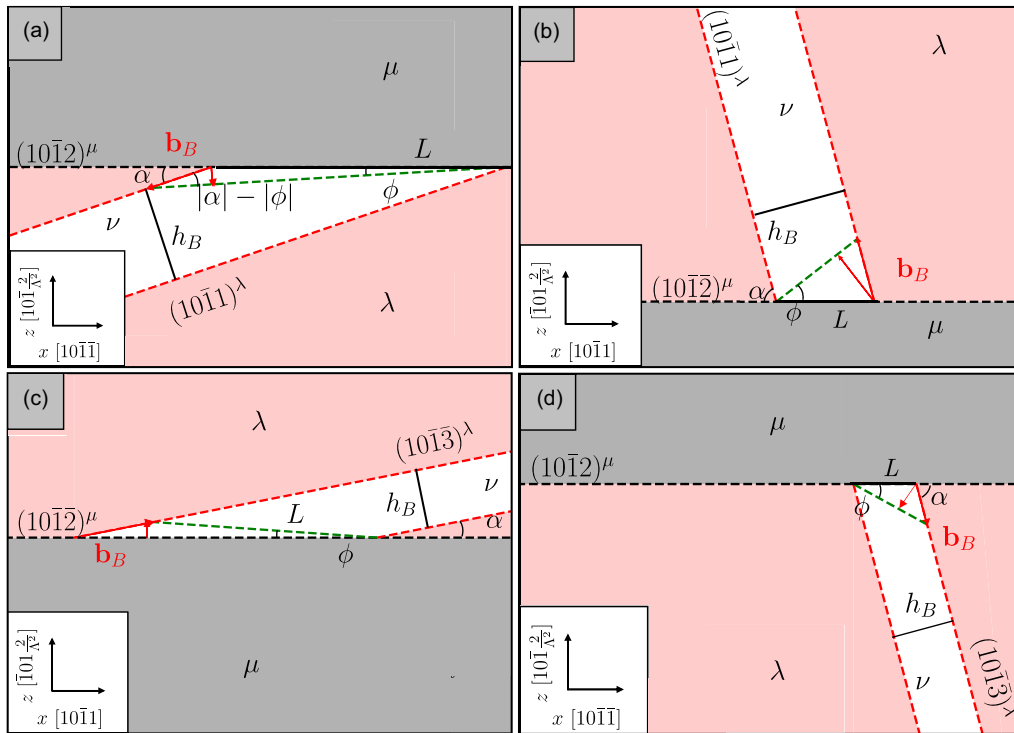


FIG. 2. Schematic of a secondary twinning disconnection with Burgers vector  $\mathbf{b}_B$  and step height  $h_B$  impinging on a flat primary twin boundary. The parent, primary, and secondary twin are denoted respectively by  $\mu$ ,  $\lambda$ , and  $\nu$ . (a)  $(10\bar{1}2) - (10\bar{1}1)$  type 1 double twin;  $L$  is the distance between the origin and the point where the top of the step meets the primary twin interface. (b)  $(\bar{1}012) - (10\bar{1}1)$  type 2 double twin;  $L$  is as in (a). (c)  $(\bar{1}012) - (10\bar{1}3)$  type 1 double twin;  $L$  (in green) is the distance between the origin and the tip of the Burgers vector. (d)  $(10\bar{1}2) - (10\bar{1}3)$  type 2 double twin;  $L$  is as in (a).

vector  $\ell$  lying in the primary  $K_1$  plane is rotated by the secondary twinning shear to position  $S_B \ell$ , and recalling that in Crocker's two-dimensional coordinate system the  $x$  axis is aligned with the  $\eta_1$  direction of the primary twin,  $\ell = [1, 0]$ . Then the angle  $\phi$  is given by

$$\phi = \cot^{-1} \left( \frac{s_B \sin \alpha \cos \alpha - 1}{s_B \sin^2 \alpha} \right). \quad (42)$$

This is different from Eq. (41), because in this formulation we are able to take into account the sign of  $\alpha$  as well as that of the twinning shear  $s_B$ , such that the correct sign is computed for  $\phi$ . Indeed, Eq. (42) yields  $\phi = -0.7^\circ$ . The same procedure can be applied to the  $(10\bar{1}1) - (\bar{1}012)$  type 2 mechanism, Fig. 1(b). In this case, the predicted rotation for the habit plane is  $\phi = 6.6^\circ$ .

A slightly different geometry is to be used for the  $(10\bar{1}3) - (\bar{1}012)$  (type 1) and  $(10\bar{1}3) - (10\bar{1}2)$  (type 2) double twinning mechanisms, due to the direction of the Burgers vector. These instances are schematically depicted in Figs. 1(c) and 1(d), where once again the length of the Burgers vectors relative to the step height has been exaggerated for clarity. In this case, our focus is the component of the Burgers vector  $\mathbf{b}_B$  perpendicular to the primary  $K_1$  plane. Then  $L$  is the distance between the origin and the tip of  $\mathbf{b}_B$  [i.e., the green dashed line in Fig. 1(c)], and we can write

$$L \sin |\phi| = b_B \sin |\alpha|, \quad (43)$$

where now  $L = |h_B| / \sin(|\alpha| + |\phi|)$ ; this can be seen by considering the triangle containing both  $\phi$  and  $\alpha$  in Fig. 1(c),

where the third internal angle is given by  $\pi - |\alpha| - |\phi|$ , such that the angle opposite  $h_B$  is  $|\alpha| + |\phi|$ . Solving Eq. (43) for  $|\phi|$ , we obtain

$$|\phi| = \cot^{-1} \left( \frac{1 - |s_B| \sin |\alpha| \cos |\alpha|}{|s_B| \sin^2 |\alpha|} \right). \quad (44)$$

Thus we find that for the  $(10\bar{1}3) - (\bar{1}012)$  double twin  $\phi = 0.3^\circ$ , while for  $(10\bar{1}3) - (10\bar{1}2)$ ,  $\phi = -7.1^\circ$ , upon examination of Figs. 1(c) and 1(d). In both cases, the angle  $\phi$  is measured relative to the  $(10\bar{1}3)$  plane of the matrix.

Similarly, the rotation of the primary  $K_1$  plane caused by the impingement of a secondary twinning disconnection can be found for the four T-C mechanisms, Fig. 2. In this case the secondary twinning disconnections with Burgers vector  $\mathbf{b}_B$  and step height  $h_B$  are those of  $(10\bar{1}1)$  and  $(10\bar{1}3)$  twinning. For the  $(10\bar{1}2) - (10\bar{1}1)$  type 1 and  $(10\bar{1}2) - (10\bar{1}3)$  type 2 mechanisms, Eq. (41) may be derived, while for the  $(\bar{1}012) - (10\bar{1}1)$  type 2 and  $(\bar{1}012) - (10\bar{1}3)$  type 1 mechanisms Eq. (44) holds. The resulting rotation angles about the normal to the plane of shear are given in Table II, along with those for the C-T mechanisms. These angles represent the maximum rotation of the double twin habit plane that can be brought about by the secondary twinning disconnections encountering a flat primary twin to matrix interface, since in the development above we have assumed that the atoms in the interface were not constrained by the matrix surrounding the twin. In practice, however, they might be constrained, and the final rotation may be smaller; if indeed all additional deformation caused by the secondary twinning shear were

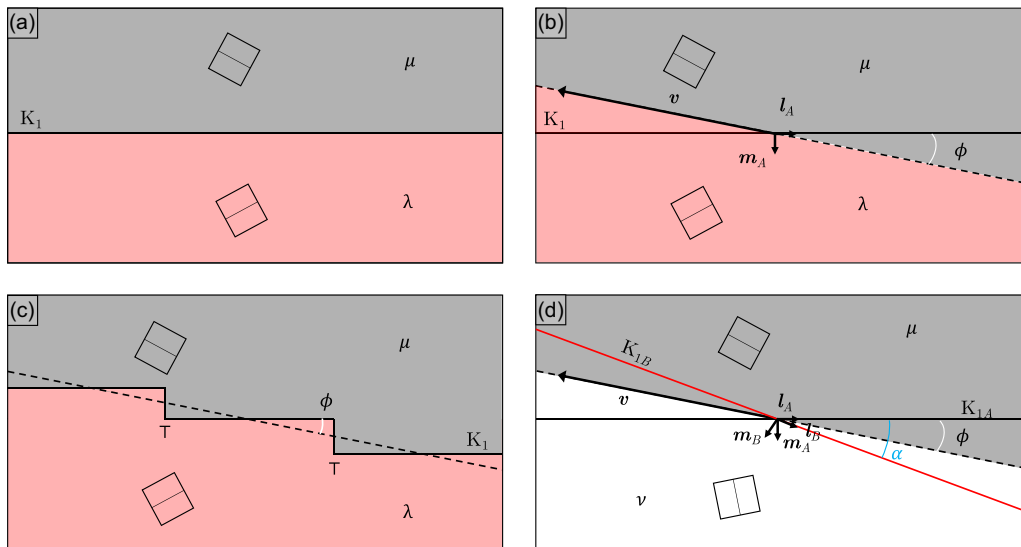


FIG. 3. Application of the Frank-Bilby equation to twin interfaces.  $\mu$ ,  $\lambda$ , and  $\nu$  denote the matrix, primary, and secondary twin respectively. (a) Commensurate twin interface with no dislocation content crossing the interface. (b) Incommensurate interface making an angle  $\phi$  with the  $K_1$  plane. (c) Dislocation content predicted by the Frank-Bilby equation for the interface in (c) resolved into twinning disconnections separating commensurate terraces of twin boundary. (d) Incommensurate interface between the matrix and the double twin. In (a) to (d), the double rectangles symbolise outlines of the hcp unit cell in matrix, twin and double twin orientations.

to be accommodated in the double twin, no rotation would be observed. Finally, the rotation might be partitioned more or less equally between the two crystals. Hence, the values reported in Table II are to be interpreted as limiting values.

It emerges from the results in Table II that for both the compression-tension and tension-compression double twinning sequences, the type 1 mechanisms lead to very small rotation angles, all a fraction of a degree. In contrast, type 2 mechanisms entail larger rotations of the habit plane by an order of magnitude; this is a consequence of the magnitude of the angle  $\alpha$  between the primary and secondary twinning planes, which is larger for the type 2 mechanisms. Therefore, the type 2 mechanisms would require more accommodation to ensure the rotation of the habit plane, which leads us to conclude that they would be less likely to occur.

### B. Mechanistic model of interfaces containing disconnections

In the previous section, we considered a fully formed primary twin with a flat commensurate interface, i.e., with no dislocation content. We now remove this constraint, and allow the primary twin interface to contain disconnections, following the approach of Karki and coworkers [28]. We then wish to know how this interface is modified by the arrival of secondary twinning disconnections, as done previously.

The dislocation content of an interface may be calculated using the Frank-Bilby equation [29,30]. If the two lattices on either side of the interface are obtained via affine transformations  $\mathbf{W}(\lambda)$  and  $\mathbf{W}(\mu)$ , the dislocation content necessary to make the lattices compatible in such a way that they would fit together at the interface is given by

$$\mathbf{b} = (\mathbf{W}(\mu)^{-1} - \mathbf{W}(\lambda)^{-1})\mathbf{v}, \quad (45)$$

where  $\mathbf{v}$  is a large vector lying in the interface, i.e., the probe vector, and  $\mathbf{b}$  is expressed in the coordinate system of the

reference lattice. As multiple descriptions of the operations  $\mathbf{W}(\lambda)$  and  $\mathbf{W}(\mu)$  exist, the characterization of an interface according to its Burgers vector density is not unique, either. A most suitable description may, however, be chosen in cases where the motion of interfacial dislocations mediates a change in the shape of the crystals: This is the case of twinning, where the glide of disconnections on the  $K_1$  plane accomplishes the growth of the twin; then the operations  $\mathbf{W}(\lambda)$  and  $\mathbf{W}(\mu)$  may be chosen to reflect how the twinning transformation is achieved [31]. Thus we choose as a description of the twinning transformation that of a simple shear, such that the dislocation description arising from the Frank-Bilby equation is that of interfacial disconnections whose task is to accomplish said shear. It may easily be seen that when the interface coincides with the  $K_1$  plane of the twin, its dislocation content is zero, as the probe vector is left invariant by the shear transformation, Fig. 3(a).

Next, we consider a different configuration, where the interface plane is at an angle  $\phi$  with the  $K_1$  plane of the primary twin, Fig. 3(b). This interface is, in general, incoherent, and the probe vector  $\mathbf{v}$ , which now lies in it is no longer invariant under a shear  $\mathbf{S}_A$ . Taking the reference lattice to be the twinned lattice  $\lambda$ , the operation  $\mathbf{W}(\lambda)$  is the identity  $\mathbf{I}$ , and the operation  $\mathbf{W}(\mu)$  is the one that transforms  $\lambda$  into  $\mu$ , expressed in the coordinate system of  $\lambda$ , i.e.,  ${}^P\mathbf{S}_A^{-1} = \mathbf{S}_A$ , where the superscript  $P$  indicates the coordinate system of the primary twin. Substituting  $\mathbf{S}_A^{-1} = \mathbf{I} - s_A \ell_A \mathbf{m}_A^T$ , where  $\ell_A$  and  $\mathbf{m}_A$  are unit vectors along  $\eta_1$  and normal to the  $K_1$  plane respectively, in Eq. (45), we find

$${}^P\mathbf{b} = (\mathbf{S}_A^{-1} - \mathbf{I})\mathbf{v} = -s_A \ell_A \mathbf{m}_A^T \mathbf{v} = s_A \sin \phi |\mathbf{v}| \ell_A. \quad (46)$$

Thus the Burgers vector content of this interface is parallel to the  $\eta_1$  direction, and we can envisage an array of twinning disconnections to make up the dislocation content. Using that for a twinning disconnection  $s_A = |\mathbf{b}_A|/h_A$ , we see that  $|\mathbf{b}_A| \ell_A =$

$\mathbf{b}_A$ , i.e., the Burgers vector of the disconnection. Defining the disconnection spacing as  $L_A = h_A/\sin\phi$  and dividing through by  $|\mathbf{v}|$ , we find the Burgers vector density

$$\frac{{}^P\mathbf{b}}{|\mathbf{v}|} = \frac{\mathbf{b}_A}{L_A}. \quad (47)$$

Although this Burgers vector content is referred to the coordinate system of the primary twin, it has the same indices in the coordinate system of the parent lattice, since the Burgers vector  $\mathbf{b}_A$  is invariant under the primary twinning shear.

Hence, this interface is formed by commensurate terraces parallel to the primary  $K_1$  plane separated by twinning disconnections, Fig. 3(c), which is consistent with the model of a lenticular twin, where loops of twinning disconnections enlarge the twin by gliding on the  $K_1$  plane, and while doing so ensure that the interface plane is locally macroscopically rotated. In the case of double twinning, however, this is a transient configuration; in fact, it is modified by the arrival of secondary twinning disconnections as the secondary twin grows inside the primary twin. These disconnections now raise the possibility that the misfit introduced by the primary twinning disconnections across the interface may be removed [28]; by misfit, we mean the net in plane Burgers vector content of the interface. The zero-misfit condition is achieved by interfacial dislocations when the total Burgers vector content parallel to the interface plane is zero [32,33], such that if the incoming secondary twinning disconnections compensate the Burgers vector content of the primary twinning disconnections parallel to the interface, the boundary plane will be free of misfit.

In order to achieve the zero-misfit condition, we first establish the Burgers vector content of an interface that makes an angle  $\phi$  with the primary  $K_1$  plane, but now separates the parent and double twin, i.e., crystals  $\mu$  and  $\nu$ , Fig. 3(d). The reference lattice is still  $\lambda$ : thus, the Frank-Bilby equation can be written as

$${}^P\mathbf{b} = (\mathbf{S}_A^{-1} - {}^P\mathbf{S}_B^{-1})\mathbf{v} = (-s_A\ell_A\mathbf{m}_A^T + s_B{}^P\ell_B{}^P\mathbf{m}_B^T)\mathbf{v}. \quad (48)$$

With the aid of Fig. 3(d), we notice that  ${}^P\mathbf{m}_B^T\mathbf{v} = \cos(\frac{\pi}{2} - \alpha + \phi)|\mathbf{v}| = \sin(\alpha - \phi)|\mathbf{v}|$ , where  $\alpha$  is the angle between the primary and secondary  $K_1$  planes. Then  $s_B = |\mathbf{b}_B|/h_B$ , such that  $|\mathbf{b}_B|{}^P\ell_B^T = {}^P\mathbf{b}_B$ . The spacing of the secondary twinning disconnections is thus given by  $L_B = h_B/\sin(\alpha - \phi)$ , such that the Burgers vector density of the interface is finally

$$\frac{{}^P\mathbf{b}}{|\mathbf{v}|} = \frac{\mathbf{b}_A}{L_A} + \frac{{}^P\mathbf{b}_B}{L_B}. \quad (49)$$

For simplicity, we now refer this Burgers vector content to the coordinate system of the matrix, such that

$$\frac{\mathbf{b}}{|\mathbf{v}|} = \frac{\mathbf{R}_A^{-1}{}^P\mathbf{b}}{|\mathbf{v}|} = \frac{\mathbf{b}_A}{L_A} + \frac{\mathbf{b}_B}{L_B}, \quad (50)$$

where  $\mathbf{R}_A$  is one of the descriptions of the transformation that relates the matrix and primary twin, e.g., a rotation by  $\pi$  about the primary  $\eta_1$  direction.

Now it is possible to apply the condition for zero misfit across the interface, i.e., that the total Burgers vector content parallel to the interface be equal to zero. This condition can only be achieved if the component of the Burgers vector of the

secondary twinning disconnection that is parallel to the vector  $\mathbf{v}$  has opposite sign to the same component of the Burgers vector of the primary twinning disconnection, i.e., if

$$\frac{|\mathbf{b}_A^\parallel|}{L_A} - \frac{|\mathbf{b}_B^\parallel|}{L_B} = 0, \quad (51)$$

where the superscript  $\parallel$  indicates the component parallel to the habit plane that makes an angle  $\phi$  with the primary  $K_1$  plane. These components are given by  $|\mathbf{b}_A^\parallel| = |\mathbf{b}_A| \cos\phi$  and  $|\mathbf{b}_B^\parallel| = |\mathbf{b}_B| \cos(\alpha - \phi)$ . Then, reintroducing  $s_A$  and  $s_B$  to simplify the expressions, Eq. (51) becomes

$$s_A \sin\phi \cos\phi - s_B \sin(\alpha - \phi) \cos(\alpha - \phi) = 0. \quad (52)$$

Solving for  $\phi$ , we find

$$\phi = \frac{1}{2} \tan^{-1} \left( \frac{s_B \sin 2\alpha}{s_A + s_B \cos 2\alpha} \right). \quad (53)$$

Thus,  $\phi$  defines a habit plane where the spacing of the primary and secondary twinning disconnections that make up its dislocation content is such that misfit across the interface is removed. We are, however, left to deal with the components of the Burgers vectors of the disconnections that are perpendicular to the interface. The Burgers vector content perpendicular to the plane that makes an angle  $\phi$  with the primary twinning plane is given by

$$\frac{\mathbf{b}^\perp}{|\mathbf{v}|} = \frac{\mathbf{b}_A^\perp}{L_A} + \frac{\mathbf{b}_B^\perp}{L_B}. \quad (54)$$

The effect of this dislocation content is to cause a rotation of the lattices relative to each other, i.e., a tilt, such that the additional rotation contributes to the macroscopic rotation of the interface [28,32]. According to the topological model, this rotational distortion field is to be partitioned equally between the two crystals in the homogeneous isotropic case [33,34]; in the case of double twinning, the crystals on either side of the interface are in the same phase and have the same elastic constants, but they are not isotropic, such that the equal partitioning of the distortion field is an approximation. Hence, if the additional tilt is given by the angle  $\psi$ , each crystal will be rotated by  $\psi/2$ , and the final orientation of the interface is given by  $\phi \pm \psi/2$  where the sign of  $\psi/2$  differs for the two crystals. If the perpendicular components of the Burgers vectors of the twinning disconnections have the same sign, the angle  $\psi$  can be found from

$$\tan\psi = \frac{|\mathbf{b}^\perp|}{|\mathbf{v}|} = \frac{|\mathbf{b}_A^\perp|}{L_A} + \frac{|\mathbf{b}_B^\perp|}{L_B}. \quad (55)$$

For small  $\psi$ ,  $\tan\psi \approx \psi$ , and we find

$$\psi = \frac{|\mathbf{b}^\perp|}{|\mathbf{v}|} = s_A \sin^2\phi + s_B \sin^2(\alpha - \phi). \quad (56)$$

Thus a misfit-free double twin interface is envisaged, where the total transformation is accompanied by a rotational distortion of the two crystals. It is, however, emphasized that as mentioned above, the condition for the misfit to be removed is that the components of the Burgers vectors of the primary and secondary twinning disconnections parallel to the interface have opposite sign. Should the parallel components have the same sign, the secondary twinning disconnections

TABLE III. Angles defining misfit-free interfaces with added rotational distortion as described by the topological model, for C-T and T-C double twin mechanisms with  $\gamma = 1.624$ .  $\phi$  is calculated using Eq. (53) and  $\psi$  is calculated using Eq. (56) (where a minus sign is introduced for the  $(10\bar{1}1) - (\bar{1}012)$  mechanism where the tilt components of the primary and secondary twinning disconnections have opposite signs). The rotation axis is the normal to the plane of shear ( $\bar{1}210$ ). Whether the misfit-free condition may be achieved for each mechanism is marked by a yes or no in the “misfit – free” row.

C-T DT	$(10\bar{1}1) - (10\bar{1}2)$	$(10\bar{1}1) - (\bar{1}012)$
	type 1	type 2
$\phi$	$-9.1^\circ$	$-7.3^\circ$
$\psi$	$0.4^\circ$	$-7.4^\circ$
$\phi + \frac{\psi}{2}$	$-8.9^\circ$	$-11.0^\circ$
misfit-free	no	yes
C-T DT	$(10\bar{1}\bar{3}) - (10\bar{1}2)$	$(10\bar{1}\bar{3}) - (\bar{1}012)$
	type 2	type 1
$\phi$	$-7.2^\circ$	$-5.4^\circ$
$\psi$	$7.1^\circ$	$-0.1^\circ$
$\phi + \frac{\psi}{2}$	$-3.6^\circ$	$-5.5^\circ$
misfit-free	no	no
T-C DT	$(10\bar{1}2) - (10\bar{1}1)$	$(\bar{1}012) - (10\bar{1}1)$
	type 1	type 2
$\phi$	$9.7^\circ$	$7.8^\circ$
$\psi$	$-0.4^\circ$	$-7.6^\circ$
$\phi + \frac{\psi}{2}$	$9.5^\circ$	$4.0^\circ$
misfit-free	no	yes
T-C DT	$(10\bar{1}2) - (10\bar{1}\bar{3})$	$(\bar{1}012) - (10\bar{1}\bar{3})$
	type 2	type 1
$\phi$	$7.7^\circ$	$5.8^\circ$
$\psi$	$7.6^\circ$	$0.1^\circ$
$\phi + \frac{\psi}{2}$	$11.5^\circ$	$5.8^\circ$
misfit-free	no	no

will only add to the misfit introduced by the primary twinning disconnections.

Hence, we now analyze the specific case of double twinning in magnesium, to understand whether misfit compensation brought about by twinning disconnections is possible. We envisage a lenticular primary twin based on the disconnection model of twinning presented above, where the macroscopic interface plane is rotated from the primary twin plane by the angle  $\phi$ . We then take a secondary twin embryo to form inside the primary twin on a plane that makes an angle  $\alpha$  with the primary  $K_1$  plane. For interfaces where misfit accommodation is possible, the angle  $\phi$  that the interface makes with the primary twinning plane can be calculated using Eq. (53), and the tilt  $\psi$  is given by Eq. (56), and the results are reported in Table III for all the C-T and T-C double twinning mechanisms.

We now consider each of these mechanisms in detail with the aid of Figs. 4 and 5. Starting from the  $(10\bar{1}1) - (10\bar{1}2)$  type 1 mechanism, Fig. 4(a), we see that the components of the Burgers vectors of the primary and secondary twinning disconnections,  $\mathbf{b}_A$  and  $\mathbf{b}_B$ , that are parallel to the interface making an angle  $\phi$  with the primary  $K_1$  plane point in the same direction. Thus, the secondary twinning disconnections add to the misfit at the interface, and misfit cancellation is not possible for this mechanism. The same holds for the  $(10\bar{1}\bar{3}) - (10\bar{1}2)$  type 2 and  $(10\bar{1}\bar{3}) - (\bar{1}012)$  type 1 twinning sequences, Figs. 4(c) and 4(d). Conversely, in the case of  $(10\bar{1}1) - (\bar{1}012)$  type 2 double twinning, Fig. 4(b), the components of  $\mathbf{b}_A$  and  $\mathbf{b}_B$  parallel to the interface have opposite sign, such that misfit cancellation may be achieved. However, it should be noted that in this case the tilt components of the Burgers vectors of the primary and secondary twinning disconnections, i.e., the components perpendicular to the interface plane, have opposite sign, such that this should be reflected by Eq. (56), and the total tilt is given by the difference of the magnitudes of these components. Applying the same analysis to the T-C double twinning sequences, we find that misfit compensation across the interface is possible

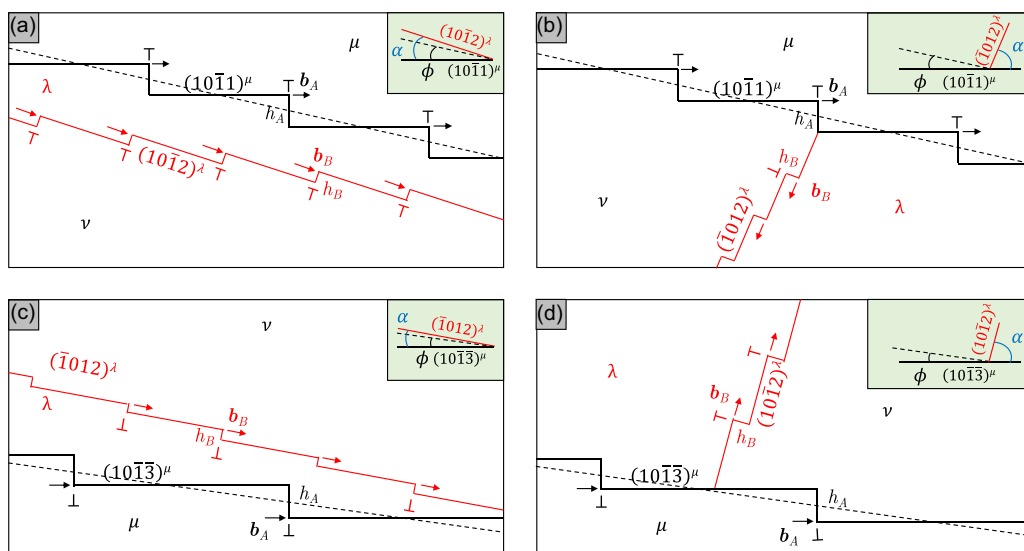


FIG. 4. Diagrams illustrating the possibility of misfit compensation across the double twin to matrix interface by combination of primary and secondary twinning disconnections for the C-T mechanisms. In (a) to (d)  $\mu$ ,  $\lambda$ , and  $\nu$  indicate the matrix, primary, and secondary twin, respectively. The projection direction is  $[1\bar{2}10]$ .

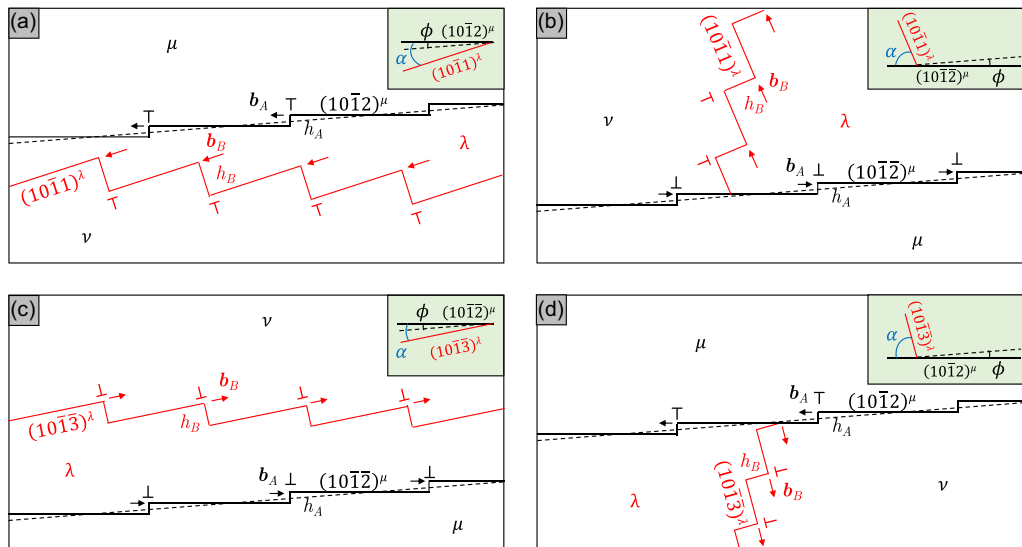


FIG. 5. Diagrams illustrating the possibility of misfit compensation across the double twin to matrix interface by combination of primary and secondary twinning disconnections for the T-C mechanisms. In (a) to (d)  $\mu$ ,  $\lambda$ , and  $\nu$  indicate the matrix, primary, and secondary twin, respectively. The projection direction is  $[1\bar{2}10]$ .

for the  $(10\bar{1}2) - (10\bar{1}1)$  type 1 [Fig. 5(b)] mechanism, while it may not be achieved for  $(10\bar{1}2) - (10\bar{1}1)$  type 2 [Fig. 5(a)],  $(10\bar{1}2) - (10\bar{1}3)$  type 2 [Fig. 5(d)] and  $(10\bar{1}2) - (10\bar{1}3)$  type 1 [Fig. 5(c)] double twinning.

The misfit-free interfaces thus obtained for the double twinning mechanisms where misfit compensation is possible are immobile, because a finite diffusive flux of atoms would be needed for the interlocked primary and secondary twinning disconnections to move, i.e., the intersection of twinning disconnections is not glissile [35]. Thus the double twin cannot grow on the habit plane defined by  $\phi + \frac{\psi}{2}$ , and is restricted to the original size of the primary twin.

## V. DISCUSSION

### A. Comparison between the topological and phenomenological models

An instructive comparison may be drawn between Crocker's model of double twinning on an invariant plane, as well as successive models of nonclassical twinning, and the topological models. It may be noted by comparing  $\phi$  and  $\phi + \psi/2$  respectively in Tables I and III that the phenomenological theory of simple shear on an invariant plane and the topological model of misfit-free interfaces yield similar results for the predicted habit planes of double twins in magnesium, although the models start from different postulates. In the phenomenological theories, it is assumed that a double twin nucleus may be able to grow on a plane left invariant by the combined shear transformations of the two twinning mechanisms. On the other hand, the topological model is based on the notion that twinning disconnections of the primary and secondary twins will arrange themselves as to eliminate misfit along the macroscopic double twin interface. However, the misfit-free condition is built into the definition of an invariant plane strain, as if an undistorted plane is picked as the interface, there is no misfit across it. Thus the topological theory

models explicitly the minimization of misfit, which is instead modelled implicitly in the phenomenological theories [28]. We have, however, seen how the premises for the achievement of a misfit-free interface by twinning disconnections exist only for some of the double twinning mechanisms under consideration, such that the construction of interfaces aligned with the predicted habit planes is not always possible.

Secondly, Crocker's theory predicts the existence of a mutual rotation between the parent and doubly twinned lattices, necessary in order to render any undistorted plane also unrotated and thus truly invariant. This rotation concerns the entirety of the doubly twinned volume, and is accommodated wholly by the parent lattice. In contrast, the topological theory imputes a local lattice distortion to the additional component of the interfacial Burgers vector content that is perpendicular to the interface, which causes the interface to tilt. This rotation is partitioned between the parent and the double twin, and for an infinite interface, the range of the distortion field is of the order of the spacing of the disconnections, and thus relatively localized [28]. Hence, although the phenomenological and topological models predict essentially the same lattice rotation, as may be seen by comparing values of  $\psi$  in Table III with those in Table I, this is a long-ranged distortion in the former case, and a short-ranged one in the latter.

Finally, the main distinction between the two models is in their treatments of the mechanisms of formation of the double twin to matrix interface. The phenomenological theory postulates that soon after the formation of a small primary twin nucleus, this retwins internally, thus becoming a double twin embryo. The double twin then expands by growing via a simple shear mechanism on a new habit plane that is an invariant plane of the double twin transformation. Conversely, according to the topological model, twin growth is the result of the motion of twinning disconnections. An array of residual primary twinning disconnections in the primary twin boundary then interacts with incoming secondary twinning disconnections, and the spacing in each array is adjusted such

that misfit across the interface may be minimized. The final interface is thus rendered immobile, and further growth of the double twin is impeded. Hence, the topological model requires that a sizable primary twin be formed first, subsequently undergoing internal retwinning that prevents any expansion of the doubly twinned volume. Indeed, if one constructs the dichromatic pattern for the double twinning modes analyzed, it is found that there are no admissible twinning disconnections that may be glissile on the misfit-free habit planes predicted by the topological model, or the invariant habit planes of Crocker's theory. It is then clear that the two models propose what may be referred to as one- and two-step processes for double twin formation: the phenomenological theory predicting that a double twin may grow on an invariant plane in one step, and the topological model envisaging the full formation of a primary twin followed by internal growth of the secondary twin in two distinct steps.

### B. Validation of theory by experiment

Experimental electron microscopy observations suggest that double twins in magnesium are created in a two-step process, with a primary twin forming first and later retwinning, as primary twins that have only partially retwinned are often reported in the literature [1,3,4,36]. This is indication that the phenomenological theories, which point to a one-step process, do not describe double twinning accurately. However, unambiguous measurement of the orientation of the double twin to matrix interface has traditionally eluded the literature, even for the most commonly occurring  $(10\bar{1}1) - (10\bar{1}2)$  type 1 variant. The most comprehensive experimental study in this sense was carried out by Cizek and Barnett [1], who studied a large number of double twins in a magnesium alloy using transmission electron microscopy, and found that the macroscopic orientation of  $\{10\bar{1}1\} - \{10\bar{1}2\}$  type 1 double twin to matrix interfaces varied between  $\{30\bar{3}4\}$ ,  $\{10\bar{1}1\}$ , and  $\{20\bar{2}3\}$ . These observations thus do not support the predictions of Crocker's model summarized in Table I. Indeed, the topological theory concludes that for this mechanism misfit compensation brought about by the secondary twinning disconnections is not possible, as the components of the Burgers vectors of the primary and secondary twinning disconnections parallel to the double twin interface do not cancel out. There is then no reason why the disconnections should be positioned as to yield an overall orientation of the interface parallel to Crocker's invariant habit planes.

Conversely, we have shown in a previous high-resolution TEM study [5] that double twin to matrix interfaces of the T-C and C-T type 1 kinds often contain facets, whose character is transformed by the action of secondary twinning disconnections but which remain otherwise commensurate, and that may be modelled using the topological theory. The facets are separated by segments of the original primary twin interface, which appear to be still aligned with the primary  $K_1$  plane. In Sec. IV A we used the topological theory to illustrate the case of secondary twinning disconnections arriving at a flat primary twin interface; it may be seen from Table II that the ensuing rotation of the double twin habit plane for type 1 mechanisms is very small, of the order of a fraction of

a degree. This is indeed consistent with the high-resolution observations, suggesting that the macroscopic orientation of the double twin to matrix interface is largely predetermined by that of the primary twin. Notably, we also showed that the results obtained for secondary twinning disconnections may be recovered by applying Crocker's secondary twinning shear to the primary  $\eta_1$  direction.

## VI. CONCLUSIONS

In this article the phenomenological and topological theories of type 1 and 2 double twinning in magnesium were presented. The findings may thus be summarized as follows.

(i) Phenomenological theories of nonclassical twinning, of which double twinning is a special case, require that double twin growth occur on an unrotated, undistorted habit plane. A simple equivalent twinning mode is thus associated with the double twin mechanism, and this may be found by either combining the primary and secondary twinning shears (Sec. III A) or the correspondence matrices associated with the individual twinning modes (Sec. III B). The resulting predicted habit planes were reported in Table I.

(ii) Two situations may be studied using the topological model. The first one is that of secondary twinning disconnections arriving at a flat primary twin interface (Sec. IV A). This produces a macroscopic rotation of the double twin to matrix interface with respect to the original primary twin plane; the magnitudes of these rotations for all double twinning mechanisms were reported in Table II. Secondly, the arrival of secondary twinning disconnections at a stepped primary twin interface may also be modelled (Sec. IV B). In this case, the twinning disconnections adjust their spacing in the double twin to matrix interfaces as to minimize misfit, if possible, thus resulting in a macroscopic rotation of the interface; results were reported in Table III.

(iii) The phenomenological model yields similar predictions to the topological model of secondary twinning disconnections minimizing misfit in a stepped primary twin interface. This is because misfit is automatically eliminated in the notion of an invariant habit plane, on which the phenomenological theory is based. However, the topological method does not require that the double twin grow as a simple twinning mode, thus allowing for a primary twin to form first, followed by internal retwinning, as supported by experimental observations.

(iv) The invariant or misfit-free habit planes predicted by both theories are not consistently observed in experimental studies of double twins. Instead, observations of type 1 double twins suggest that the orientation of the double twin to matrix interface is mostly predetermined by that of the primary twin interface, sustaining the predictions of the topological model of secondary twinning disconnections impinging on a flat primary twin interface.

## ACKNOWLEDGMENTS

We thank R. C. Pond for helpful and stimulating discussion. M.R. is funded by a studentship in the EPSRC Centre for

Doctoral Training, CANES, under Grant No. EP/L015854/1. We are grateful for funding by Luxfer (MEL) Technologies

and we thank Dr. Matthew Murphy for support. A.T.P. is funded under the MATLeS EPSRC Grant No. EP/V001787/1.

- 
- [1] P. Cizek and M. R. Barnett, *Scr. Mater.* **59**, 959 (2008).
- [2] M. R. Barnett, Z. Keshavarz, A. G. Beer, and X. Ma, *Acta Mater.* **56**, 5 (2008).
- [3] E. Martin, L. Capolungo, L. Jiang, and J. J. Jonas, *Acta Mater.* **58**, 3970 (2010).
- [4] X. An, S. Ni, and M. Song, *Philos. Mag. Lett.* **99**, 21 (2019).
- [5] M. Ruffino, J. Nutter, X. Zeng, D. Guan, W. M. Rainforth, and A. T. Paxton, *Sci. Rep.* **13**, 3861 (2023).
- [6] D. Guan, W. M. Rainforth, L. Ma, B. Wynne, and J. Gao, *Acta Mater.* **126**, 132 (2017).
- [7] D. Guan, X. Liu, J. Gao, L. Ma, B. P. Wynne, and W. M. Rainforth, *Sci. Rep.* **9**, 7152 (2019).
- [8] R. W. Cahn, *Adv. Phys.* **3**, 363 (1954).
- [9] B. A. Bilby and A. G. Crocker, *Proc. R. Soc. London A* **288**, 240 (1965).
- [10] A. G. Crocker, *Philos. Mag.* **7**, 1901 (1962).
- [11] M. Bevis and A. G. Crocker, *Proc. R. Soc. London A* **304**, 123 (1968).
- [12] M. Bevis and A. G. Crocker, *Proc. R. Soc. London A* **313**, 509 (1969).
- [13] J. W. Christian and S. Mahajan, *Prog. Mater. Sci.* **39**, 1 (1995).
- [14] J. W. Christian, *The Theory of Transformations in Metals and Alloys*, International series on materials science and technology (Elsevier Science, Amsterdam, 2002).
- [15] J. W. Christian, *The Theory of Transformations in Metals and Alloys (First edition)*, International series on materials science and technology (Elsevier Science, Amsterdam, 1965).
- [16] A. J. McConnell, *Applications of Tensor Analysis*, Dover Books on Mathematics (Dover Publications, New York, 1957).
- [17] A. B. Acton, M. Bevis, A. G. Crocker, and N. D. H. Ross, *Proc. R. Soc. Lond. A* **320**, 101 (1970).
- [18] A. G. Crocker, F. Heckscher, M. Bevis, and D. M. M. Guyoncourt, *Philos. Mag.* **13**, 1191 (1966).
- [19] A. T. Paxton and A. R. Entwisle, *Philos. Mag. A* **52**, 573 (1985).
- [20] J. P. Hirth and R. C. Pond, *Acta Mater.* **44**, 4749 (1996).
- [21] R. C. Pond, J. P. Hirth, A. Serra, and D. J. Bacon, *Mater. Res. Lett.* **4**, 185 (2016).
- [22] R. C. Pond and D. S. Vlachavas, *Proc. R. Soc. Lond. A* **386**, 95 (1983).
- [23] R. C. Pond, *MRS Proceedings* **122**, 49 (1988).
- [24] R. C. Pond and F. R. N. Nabarro (eds.), *Dislocations in Solids* (North-Holland, Amsterdam, 1989), Vol. 8.
- [25] A. Serra, D. J. Bacon, and R. C. Pond, *Acta Metall.* **36**, 3183 (1988).
- [26] A. Serra, R. C. Pond, and D. J. Bacon, *Acta Metall. Mater.* **39**, 1469 (1991).
- [27] R. C. Pond, D. J. Bacon, A. Serra, and A. P. Sutton, *Metall. Trans. A* **22**, 1185 (1991).
- [28] B. Karki, P. Müllner, and R. Pond, *Acta Mater.* **257**, 119131 (2023).
- [29] F. C. Frank, *Symposium on the Plastic Deformation of Crystalline Solids* (Office of Naval Research, Pittsburgh, Pennsylvania, 1950), p. 150.
- [30] B. A. Bilby, *Report on the Conference on Defects in Crystalline Solids* (The Physical Society, London, 1955), p. 123.
- [31] A. P. Sutton and R. W. Balluffi, *Interfaces in Crystalline Materials*, Monographs on the Physics and Chemistry of Materials (Clarendon Press, New York, 1996).
- [32] J. P. Hirth, R. C. Pond, R. G. Hoagland, X.-Y. Liu, and J. Wang, *Prog. Mater. Sci.* **58**, 749 (2013).
- [33] J. P. Hirth and R. C. Pond, *Philos. Mag.* **90**, 3129 (2010).
- [34] J. Wang, J. P. Hirth, R. C. Pond, and J. M. Howe, *Acta Mater.* **59**, 241 (2011).
- [35] R. C. Pond and S. Celotto, *Int. Mater. Rev.* **48**, 225 (2003).
- [36] D. Ando, J. Koike, and Y. Sutou, *Acta Mater.* **58**, 4316 (2010).